Hindawi
Mathematical Problems in Engineering
Volume 2018, Article ID 8043526, 15 pages
https://doi.org/10.1155/2018/8043526

Research Article

Debris Recognition Methods in the Lubrication System with Electrostatic Sensors

Huijie Mao, Hongfu Zuo, Han Wang, Yibing Yin, and Xin Li

College of Civil Aviation, Nanjing University of Aeronautics and Astronautics, Nanjing 210016, China

Correspondence should be addressed to Huijie Mao; maohuijie0709@163.com

Received 10 April 2018; Revised 3 November 2018; Accepted 26 November 2018; Published 20 December 2018

Academic Editor: Mohammed Nouari

The oil-line electrostatic sensor (OLS) is a developing debris monitoring sensor. Previous work has shown that electrostatic charge signals can indicate the debris by calculating the Root Mean Square (RMS) value or the correlation-based indicator, but the precision of these methods is not high. This paper further developed the more accurate methods to obtain detailed debris information. Firstly, to interpret the monitoring principle of OLS and provide the guidance for developing the debris recognition methods, this paper analyzed the possible charge sources in the lubrication system and obtained the characteristics of the OLS by establishing its mathematical model. Further, a new OLS test rig was designed and verified the correctness of the sensor's characteristics and its mathematical model. Based on the characteristics of the sensor, two new debris recognition methods were proposed. Finally, the effects of the new debris recognition methods were verified by the practical industrial gearbox bench test. Results showed that, compared to the traditional methods, the new methods could recognize the debris effectively and provide more detailed information of the debris.

1. Introduction

Oil monitoring of lubrication system is an important way to monitor the friction pairs, such as bearings and gears [1]. The traditional methods of oil monitoring are most off-line, such as ferrograph, spectrometric oil analysis, and optical microscopy [2]. However, with the development of Prognostics and Health Management (PHM), on-line condition monitoring systems become the essential requirement of the PHM for important components. The use of chip detectors and inductive devices makes the on-line oil monitoring a reality. Whereas due to the restrictions of their monitoring principles, chip detectors are incapable of capturing nonferrous debris and inductive devices are also insensitive to smaller particulate and nonferrous debris. Some researchers have been improving the detection capability of the inductive sensor [3, 4], but nowadays the detection range of the mature inductive devices is typically >100 μm ferrous and >250 μm nonferrous debris in practical application [5, 6]. With the application of new nonferrous materials in friction pairs, such as the ceramic bearing, these kinds of sensors will not be able to monitor them effectively. To solve these problems, the oil-line electrostatic sensor (OLS) was developed.

Wood from the University of Southampton first proposed the electrostatic induction method at the World Tribology Conference in 1997 trying to monitor the oil-lubricated gear gluing or adhesive wear [7, 8]. The basic principle is that the debris produced by the failure of components in the oil system will carry a certain amount of charge, which will be monitored by the electrostatic sensor according to the principle of electrostatic induction [9]. In past decades, the effectiveness of oil debris monitoring has been proved by the successful applications of ferrography technologies and inductive transducers. Monitoring of the debris, especially the tiny debris, can indicate the onset of failures. Researches have shown that in the laboratory the OLS is sensitive to sub 20 μm metallic or nonmetallic debris [10]. As a new debris monitoring technology, the OLS is still under development. The challenges mainly focus on the mechanism of charge generation in the lubrication system, the characteristics, and the industrial application of the sensor.

A series of experiments were designed and attempt to explain the mechanism of charge generation in the lubrication system. Through experiments, Harvey found the debris produced by adhesive wear to be positively charged and the magnitude of charge was directly related to the total volume loss [11]. Wood presented an experimental investigation into the effect of lubricating oil quality on tribo-charging, which indicated that the oil flow would also carry some charge [12]. In addition, Harvey designed a test rig and studied the effects of oil chemistry on the charging ability of various oils [13]. Morris investigated how component material affected the charge mechanisms [6]. Also, Ling Wang conducted research on ceramic material and the quantitative relationship between charge level and wear volume [14].

Compared with the study of the charge generation mechanism in the lubrication system, there is much less research on the sensor system itself, such as the model and the sensing characteristics of the sensor. However, in other areas, there are some similar studies. In the field of gas-path electrostatic monitoring, Honor proposed a simple equation of a rob-shaped electrostatic sensor to indicate the relationship between the measured charge and the real signal [15]. Chen established a model of a plate-shaped electrostatic sensor and analyzed the sensor's sensing characteristics [16]. Addabbo T studied the effects of conditioning circuits on the signal waveforms, which provided guidance for building a suitable electrostatic sensor acquisition circuit [17]. In the field of gas-solid two-phase flow measurement, Zhang established a mathematical model of the strip-shaped electrostatic sensor [18]. Although some methods and ideas from other areas can be referenced, due to the different sensor structures and the different application situations between the OLS and other kinds of electrostatic sensors, to understand the OLS in-depth, it is necessary to investigate the detail mathematical model for the OLS and derive its own sensing characteristics theoretically to provide guidelines for the application.

In the field of OLS application, the most famous experiment is the engine test conducted by Pratt and Whitney [9]. Two F100 seeded fault engine tests (SFETs) were provided to explore the practical application of OLS. However, in this experiment, the sensor did not really detect the debris [15], whereas an application in the wind turbine gearbox achieved a relatively good result [19]. In addition, several laboratory-based simulation experiments also obtained good measurement results, such as the FZG test carried out by Harvey [12] and the bearing rig test conducted by Harvey [5]. The different measurement environments may lead to the differences of the results, and obviously the practical industrial environment is more challenging for the OLS. What is more, the signal analysis method is also one of the limitations for the application of the OLS. From the existing researches, there are two main analysis methods for electrostatic signals: monitoring the RMS value of the output signal and calculating the cross-correlation function between the dual sensing elements in the sensor. Powire put forward these two methods and applied them in the signal processing of an engine bench test and an FZG gear scuffing test [6, 9, 10]. Subsequently, Chen et al. applied these two methods in the rolling element bearings anomaly monitoring [20, 21]. Harvey also used the RMS value as a feature to indicate the health condition of the rolling element bearings [5]. In these applications, the two methods achieved some effects but did not reach the level of individual debris recognition. Moreover, the RMS value of OLS may be load-dependent as well being influenced by working condition of the oil. Furthermore, for correlation-based method, it is insensitive for the situation when the debris is tiny and the amount of debris is few. Mao tried another method based on the pulse recognition, but the method needs more theoretical proof and effect tests [19]. Therefore, it is necessary to continue to extract more efficient features to indicate the generation of the debris, especially the features suitable for the practical application environment.

To summarize, it can be seen from the above reviews that although the mechanisms of charge generation in the oil system are still not fully understood, it is believed that the debris will carry a certain amount of charge in the lubricating oil system. The characteristics of the OLS are essential to the application of the sensor, but only a few articles have been reported, which needs further research. Although several simulation experiments have been carried out, including the engine bench experiment, the data analysis methods did not reach the level of debris recognition. Some researchers proposed the correlation-based and RMS-based parameters to characterize the debris, but their physical meanings are unclear and the effects are not so good, which leads to the limitation of the sensor's applications.

This study aims to improve the oil-line electrostatic monitoring technology further and try to solve the above problems by detailing the research on the characteristics of the sensor and its recognition methods of debris. To this end, by constructing the detailed mathematical model of the OLS, the characteristics of the sensor and its change rules were analyzed in-depth first, which could provide the guidance for developing the debris recognition method. Then, a new OLS calibration device was constructed by creatively using a charged oil droplet to simulate the charged abrasive debris, which has the ability to verify the established mathematical model and the correctness of the derived sensor characteristics. Thirdly, according to the characteristics of the sensor signal, a new method for identifying abrasive particles suitable for practical applications and an abnormal monitoring method based on electrostatic signals are proposed. Moreover, with the practical industrial gearbox bench test, the proposed new methods along with the traditional methods for debris recognition are analyzed and compared. The rest of this paper is organized as follows. In Section 2, this paper researches the principle of the sensor by analyzing the possible charge sources in the oil system, establishing the mathematic model and deducing the characteristics of the sensor from the model. In Section 3, an OLS test platform is designed to validate the correctness of the performance and the mathematic model of the sensor. In Section 4, based on the characteristics of the sensors, two new methods are proposed to recognize the debris. In addition, a practical application of the sensor in the industrial gearbox is carried out to verify the feasibility of OLS and its debris recognition methods. Conclusions are drawn in Section 5.

2. The Principle of OLS

The research on the principle of OLS mainly includes the study of the charge generation mechanism in the lubrication system and the sensor's characteristics, while establishing the mathematical model of OLS is a good way to determine its characteristics. Therefore, this section will discuss the three parts separately.

2.1. Charge Generation Mechanisms. To detect the debris successfully, the electrostatic monitoring technology under the lubrication condition requires an in-depth study of the charging mechanism of the debris and the analysis of other possible charge sources in the oil system. The exact physical reasons for these charge generation events are still under investigation, but evidence shows that they are linked to the onset of debris formation and tribo-charging [22].

When the lubrication failure or oil film rupture occurs, the friction surface will contact directly. In severe cases, gluing will occur and lead to destructive failure damage. During this case, the touching asperities adhere together, and the plastic shearing removes the tip of the softer asperities, leaving them adhering to the harder surface. Subsequently, the asperities are detached and contribute to the generation of debris [11, 23]. In this process, the formation of debris is accompanied by energetic shearing and requires the breaking of multiple atomic bonds resulting in a net charge on the parent surface and the detached material [11]. This debris' charge is related to the physical nature of the detached material and the properties of the surrounding medium. Also, the morphology of the debris such as the size will influence the charge. Studies have shown that the charge density of debris can reach 3×10^{11} e/cm^3. Taking a debris with a diameter of 100 μm as example, it will carry a charge of 10 pC [24].

In the lubrication oil system, besides the formation of debris accompanied by the generation of charge, studies show that the oil's relative motion over a solid surface will also lead the oil to carry some charge, which is a well-known electrochemical concept named tribo-charging [25]. There is a double layer existing in the interface of the metal and the low conductivity oil. The oil layer closest to the metal's surface consists of either all positive or all negative charges. When low conductivity oil flows over the solid surface, the relative motion will lead a portion of double layer to be stripped and entrained into the oil flow and thus generate free electrostatic charge in the oil flow. However, the charge density generated during the flow of the lubricant is low [22]. In addition, the oil system is usually stable, so the tribo-charge is also relatively constant. Therefore, the oil charge is considered as the background signal of the OLS. With the degradation of oil, the overall background charge level will change. Typically, charge levels will reduce with the oil degradation [15]. This is also the potential for OLS to monitor the oil degradation.

2.2. The Mathematic Model of the Sensor. As Figure 1 shows, the structure of the OLS consists of metal annular electrode, insulator, shield cover, and signal acquisition system. According to the principle of electrostatic induction, when the charged debris passes through the sensor, it will generate the induced charge on the metal electrode, and the quantity of the induced charge can be obtained through the acquisition circuit as shown in the right part of Figure 1. The induced charge on the electrode is amplified by the charge amplifier and converted into the analog voltage signal. Then through the A/D conversion circuit, the analog signal is converted into a digital signal and stored into the computer for further processing. Due to the principle of the charge amplifier, the measured voltage signal has a linear relation with the original charge signal.

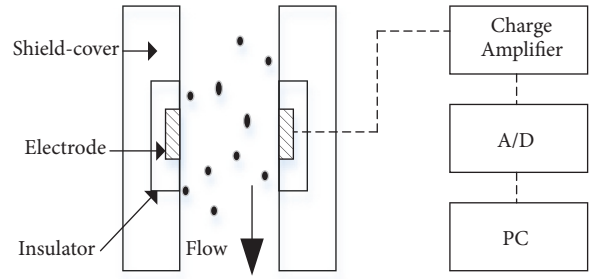

Figure 1: The structure of OLS.

To understand the characteristics of the electrostatic sensor deeply, the relationship between the debris charge and the electrostatic sensor signal needs to be further studied, which can be easily obtained by establishing the sensor's mathematical model. Based on the physical structure shown in Figure 1, the mathematical model of the sensor can be established as follows. In practice, the amount of debris passes through the sensor each time is not constant, since the amount could be single or multiple. But according to the superposition principle, the case of multiple debris can be obtained by superimposing the case of single debris, so the model in this paper is established only for the case of single debris and given that the debris can be considered as a point charge.

Firstly, to build the model, the spherical coordinate system was established as shown in Figure 2. The coordinate system takes the axis direction of the ring-shaped sensor as the zenith direction, the plane orthogonal to the zenith, and contained the point charge as the XOY plane and the intersection of XOY plane and Z axis as the origin. In the XOY plane, the point charge is located at the position $(\rho, \varphi, 0)$ ($0 \le \rho <$ R, R represents the radius of the sensor). In the XOZ plane, a microelement sensing region denoted by ds is taken from the electrode, whose coordinate is $(r, 0, \theta)$. So, the distance r' from ds to the point charge is

$$r' = \sqrt{R^2 + \rho^2 - 2R\rho\cos\varphi + R^2\cot^2\theta} \tag{1}$$

By Coulomb's law, the electric field intensity at ds denoted by dE can be obtained:

$$\begin{aligned} \mathrm{d}E &= \frac{q}{4\pi\varepsilon_0 r'^2} \\ &= \frac{q}{4\pi\varepsilon_0\left(R^2 + \rho^2 - 2R\rho\cos\varphi + R^2\cot^2\theta\right)} \end{aligned} \tag{2}$$

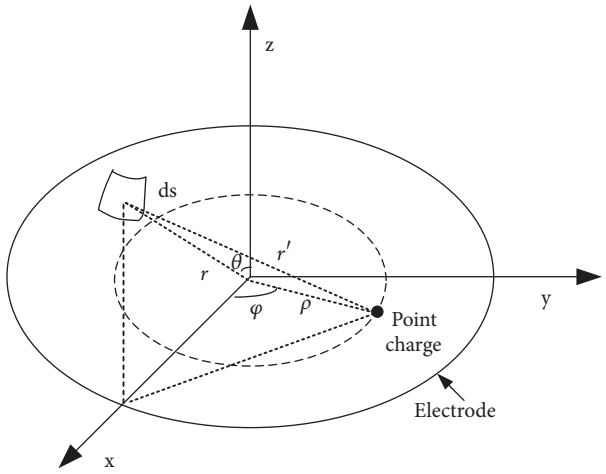

Figure 2: Spherical coordinate system.

where ε_0 is the vacuum dielectric constant; q is the charge of the point charge. According to Gaussian theorem, the charge dq_s induced by the point charge at ds is

$$dq_s = -\varepsilon_0 dE_V dS \tag{3}$$

where dE_V is the component of dE perpendicular to the surface of the element, since only the vertical component has a role in the generation of the induced charge. dS is the surface area of the microelement: $dS = r d\theta R d\varphi$. According to (1), (2), and (3), dq_s can be obtained as

$$dq_s = -\frac{q \bullet (R - \rho \bullet \cos\varphi)}{4\pi \left(R^2 + \rho^2 - 2R\rho\cos\varphi + R^2\cot^2\theta\right)^{3/2}} \bullet \frac{R}{\sin\theta} d\theta \bullet R d\varphi \tag{4}$$

The charge dq_c generated by the point charge in the annular electrode with the polar angle θ is

$$dq_c = \int_0^{2\pi} -\frac{q \bullet R^2 \bullet (R - \rho \bullet \cos\varphi)}{4\pi \sin\theta \left(R^2 + \rho^2 - 2R\rho\cos\varphi + R^2\cot^2\theta\right)^{3/2}} d\theta\, d\varphi \tag{5}$$

To get the entire induced charge on the electrode, a new coordinate system was established, whose origin is the center of the probe and reference plane is the cross section, as shown in Figure 3. In the new coordinate system, the height of the electrode is 2b and the coordinate of point charge is (ρ_x, ρ_y, z_0), where ρ_x, ρ_y are the projections in X and Y axis of the point charge. So, in the spherical coordinate system, the range of the polar angle of ds can be expressed as

$$(\theta_{\min}, \theta_{\max}) = \left(\frac{\pi}{2} - \arctan\frac{b - z_0}{R}, \frac{\pi}{2} + \arctan\frac{b + z_0}{R}\right) \tag{6}$$

Subsequently, the induced charge on the entire electrode is

$$Q = \int_{\theta_{\min}}^{\theta_{\max}} \frac{dq_c}{d\theta} d\theta \tag{7}$$

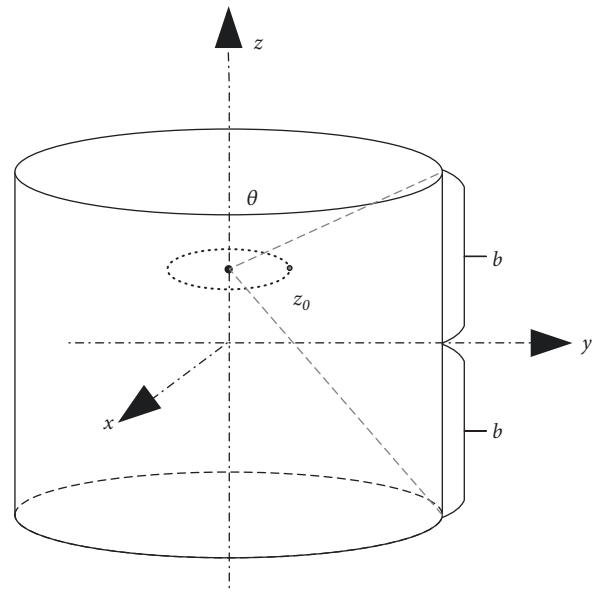

Figure 3: The relative position of point charge and electrode.

Substituting (5) into (7), the induced charge on the electrode is

$$Q = -\int_{\theta_{\min}}^{\theta_{\max}} \int_0^{2\pi} -\frac{q \bullet R^2 \bullet (R - \rho \bullet \cos\varphi)}{4\pi \sin\theta \left(R^2 + \rho^2 - 2R\rho\cos\varphi + R^2\cot^2\theta\right)^{3/2}} d\varphi\, d\theta \tag{8}$$

Equation (8) is the mathematical model of the sensor. Through the mathematical model, when the debris passes through the sensor, the output waveform of the sensor can be simulated as shown in Figure 4. It can be seen that the amplitude and the pulse width are two important parameters of the debris' signal. For the convenience of identification, the pulse width is defined as the time between the points with the value of 0.1 amplitude [26, 27]. Specifically, because of the symmetry of the sensor structure, the amplitude of the signal occurs in the position where the debris pass through the center cross section of the electrode. Therefore, the study of OLS's characteristics in this paper mainly focuses on the change rules of the amplitude and pulse width of the signal.

2.3. Relationship between the Debris and Output Signals. Since this paper studies the identification method of debris, it is not necessary to consider the influence of the sensor's structural parameters in the model. For the sensor whose structural parameters have been determined, the induced charge is only related to the characteristics of debris (radial position, speed, and charge). With the mathematical model, we can simulate the corresponding relationships qualitatively. In this paper, the electrode's length and radius of the sensor for simulation analysis are 70mm and 19mm, respectively.

2.3.1. The Relationship between the Charge of the Debris and the Signal. From the mathematical model (8), we can draw the following formula: $Q = K \times q$, where K is a function

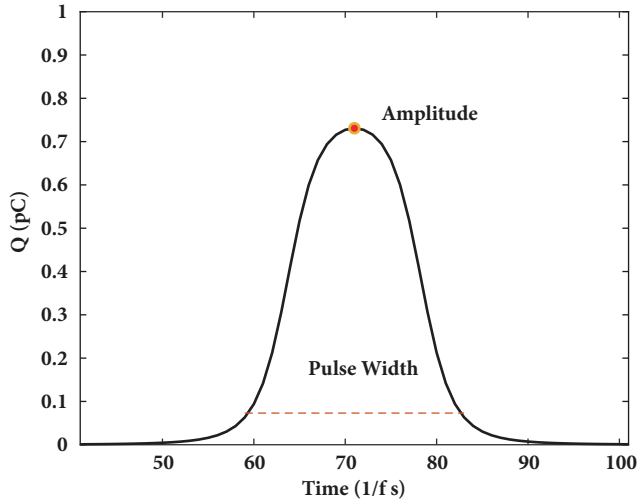

FIGURE 4: The simulated signal waveform.

independent of the point charge q. It is obvious that, in the constant radial position and speed, the signal's amplitude is proportional to the charge of the debris. Through simulating the outputs when the $q = \mathrm{n} \times q_0$ ($\mathrm{n} = 1, 2, \ldots, 8$, $q_0 =$ 1pC), respectively, the results were shown in Figure 5. From simulation results and the mathematical model, it can be concluded that, in the same radial position and speed, (1) the amplitude of the signal increases linearly with the increase of the debris' charge; (2) since the signal waveform is amplified as a whole, the pulse width does not change with the debris' charge.

2.3.2. The Relationship between the Radial Position and the Signal. In model (8), the relationship between the output signal Q and the radial position of the debris is not simply linear. However, the numerical calculation can be used to qualitatively simulate the relationship. The simulated signals in radial position $r = \{0, 0.002, 0.004, \ldots, 0.016, 0.018$ mm$\}$ are shown in Figure 6.

It can be seen from Figure 6 that if the speed and charge of the debris remain constant, (1) the closer the debris is to the wall of the electrode, the greater the amplitude of the signal is; (2) the closer the debris is to the wall, the smaller the width of the signal is. In particular, the relationship between the width and position can be fitted by quartic polynomial.

2.3.3. The Relationship between the Velocity of the Debris and the Signal. In model (8), $v \times t$ can be regarded as the position of the debris in the Z-axis direction. Based on this, model (8) can be transformed into $Q = f(z)$, where $f(z)$ is a function independent of the speed and time. The essence of the pulse width is the time the debris passes through the points of 0.1 amplitudes. The points induced 0.1 amplitudes which are fixed, so if the speed is different, the elapsed time is different, that is, the pulse width is different. Therefore, from the mathematical model, the speed of debris only affects the pulse width and does not affect the amplitude of the signal. At the same radial position, simulations were carried out on the speeds $\mathrm{n} \times v$ ($\mathrm{n} = 1, 1.2, 1.4, \ldots, 2.8$, $v = 2.96$ m/s). The results are shown in Figure 7. It can be concluded that, in the same radial position, (1) as the debris' speed increases, the pulse width will decrease, and specifically they obey the inversely proportional relationship; (2) the amplitude does not change with the speed.

Through the above analysis, the characteristics of the sensor can be concluded. Firstly, the amplitude of the signal has a proportional relationship to the charge of the debris and a nonlinear relationship with the radial position of debris. The amplitude of the signal has nothing to do with the flow rate and specifically, the relationship between the amplitude of the signal Q_a and the charge of the debris q can be measured by the sensitivity of the sensor, which is defined as $Sen = Q_a/q$ and can be obtained by calibration experiments. Secondly, the pulse width of the signal is related to the velocity and radial position of the debris, and when the radial position is constant, the pulse width is inversely proportional to the speed. When the velocity is constant, the pulse width decreases nonlinearly with the radial position.

3. Verification Experiments in the Laboratory

In order to verify the correctness of the mathematical model of the sensor and the characteristics derived from it, an OLS verification test rig was designed, which can also be used to calibrate the sensor further. With the test rig, three sets of experiments were carried out to verify the relationship between the input and the output of the sensor in three different conditions, which were different sensory charge, different positions and different speeds.

3.1. The Test Rig. As Figure 8 shows, the test rig consists of an oil drop generation and charge section, a sensor support and positioning section, an electrostatic signal acquisition section, and an oil drop charge measurement section. The oil droplet charge section mainly includes the oil tank, valve, metal needle, ring electrode, and DC adjustable power supply. When the device works, through the valve the lubricating oil in the oil tank enters the high voltage electric field formed by the metal needle and the annular electrode. Under the action of the high voltage electric field, the oil droplets will carry a certain amount of charge. The high voltage electric field strength can be adjusted by the adjustable DC power supply, the maximum output voltage of which is 500 V. The relationship between the charge of the oil droplets and the applied voltage can be expressed by the formula: $Q_{oil} = CU$, where C is the capacitance of the oil droplet, U is the applied voltage, and it is obvious that the charge quantity Q_{oil} of the oil droplet is proportional to the voltage U. Therefore, the test rig can adjust the charge through changing the voltage linearly. The sensor support and position section can accurately adjust the relative position between the center axis of the sensor and the drop path of the oil drop through the slide rail and also the altitude of the sensor to adjust the speed when the oil drops pass through the sensor. The output signal of the sensor can be obtained in real time with NI acquisition card in the signal acquisition section. The charge measurement

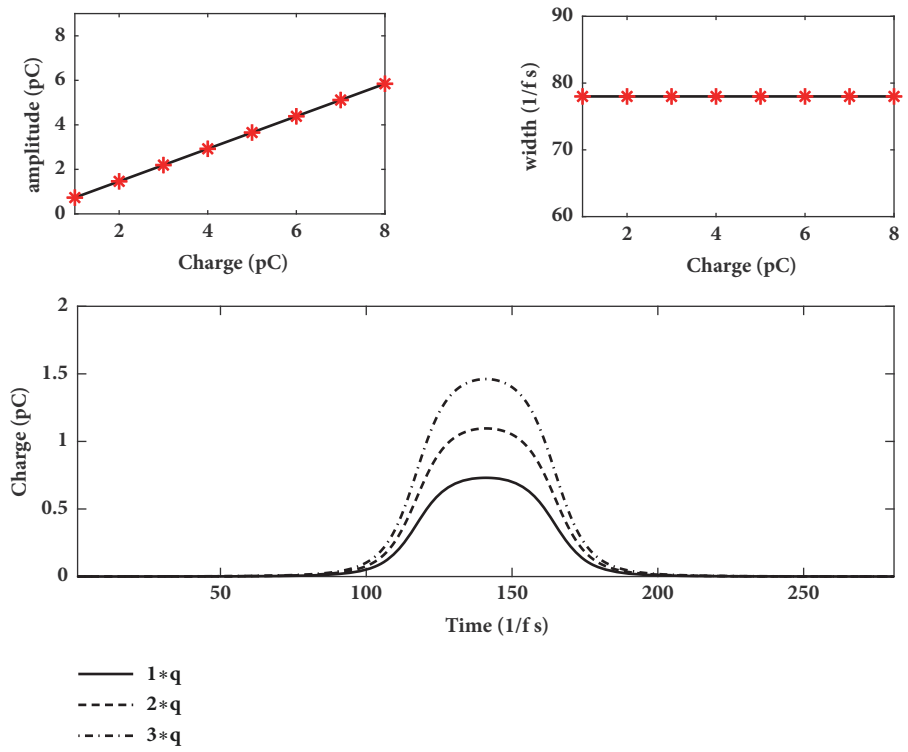

Figure 5: The relationship between the debris charge and the signal.

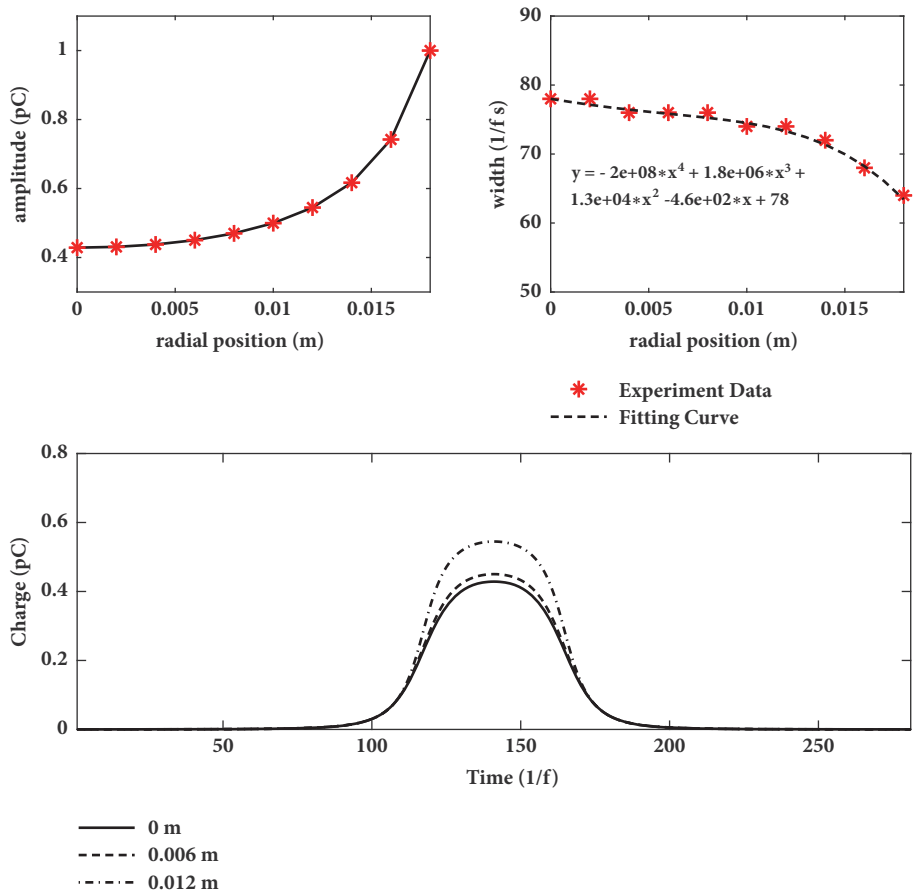

Figure 6: The relationship between radial position and signal.

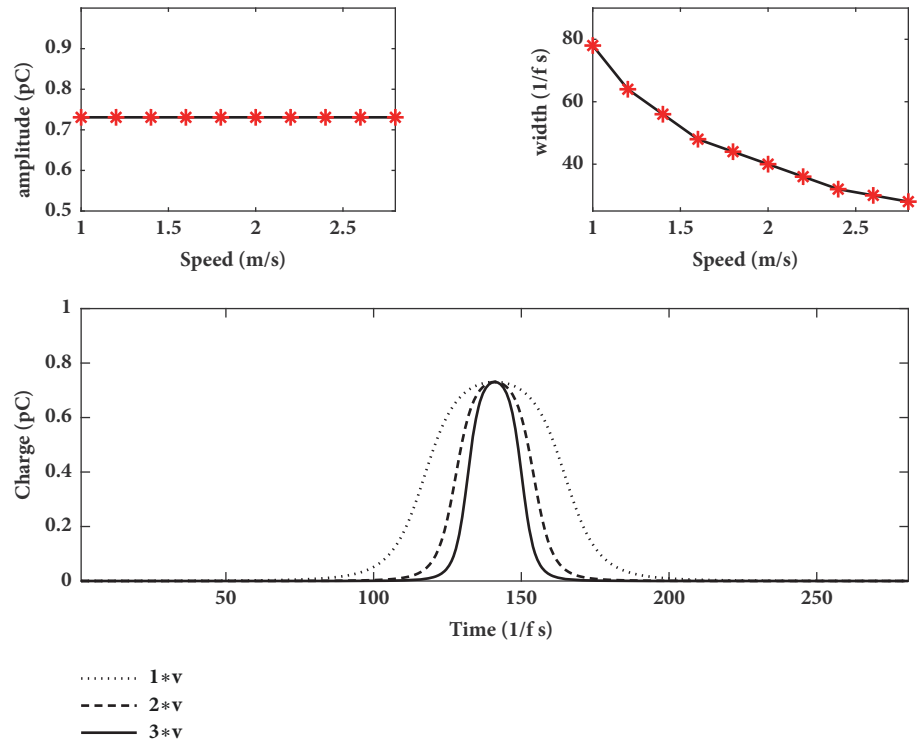

Figure 7: The relationship between the velocity of the debris and the signal.

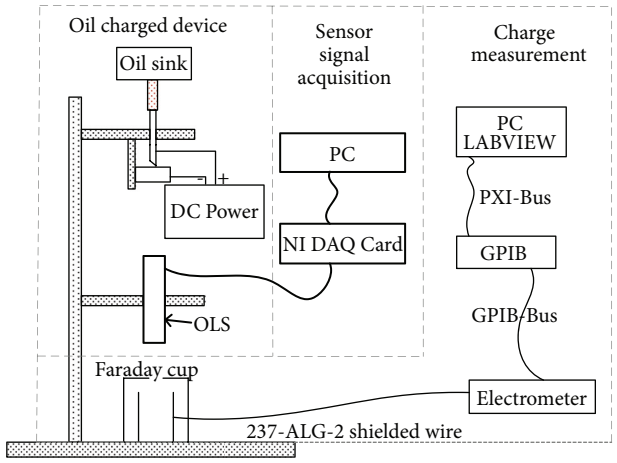

Figure 8: The calibration test rig.

section measures the exact charge of the oil droplets by means of a Faraday cup and a Keithley 6517B electrometer with a resolution up to 0.01 pC.

3.2. The Experiments

3.2.1. Different Input Charge. Different voltages were applied to the oil drop generation and charge device to produce oil droplets with different charge. The voltage increased from 0 to 500V with the step 50V. The equivalent speed of the oil droplets was set to 2.96 m/s. The outputs of the Faraday Cup and the electrostatic sensor are shown in Figures 9 and 10 respectively. The small red box in Figure 9 represents the measured data point and the dotted line is the fitting curve. It was proven from the fitting curve that the charge of the oil droplets produced by the device was proportional to the applied voltage, which was consistent with the theoretical model. As shown in Figure 10, the actual signal's waveform was also consistent with the waveform calculated by the mathematical model. Therefore, the amplitude and pulse width of the signal can be extracted as features. Figure 11 showed that the relationship between the actual amplitude of the signal and the oil droplet's charge was linear, while the relationship between the pulse width and the oil droplet charge was basically unchanged. In particular, the width of the experiment agreed with the simulation results in Figure 5 very well.

3.2.2. Different Radial Positions. As can be seen from model (8), in different radial positions, the sensor output is different. To prove this, the DC power supply voltage and the oil droplet equivalent speed were set to 300 V and 2.96 m/s respectively, and the output of the sensor was measured at the radial position $\{0, 4, 8, 12, 16, 18 \text{ mm}\}$. The results in Figure 12 showed that, as the charged oil droplet got closer to the wall, the amplitude of the signal became higher, while the pulse width became shorter, which were consistent with simulation results. Meanwhile, the width also obeyed the fitting curve obtained by simulation result in Figure 6.

3.2.3. Different Velocities. To verify the effect of speed on the electrostatic signal, the supply voltage was set to 300 V and

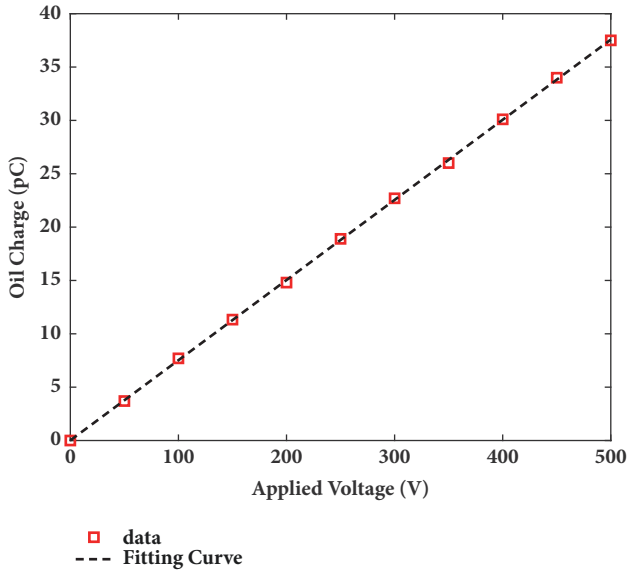

Figure 9: The relationship between the oil droplet charge and the applied voltage.

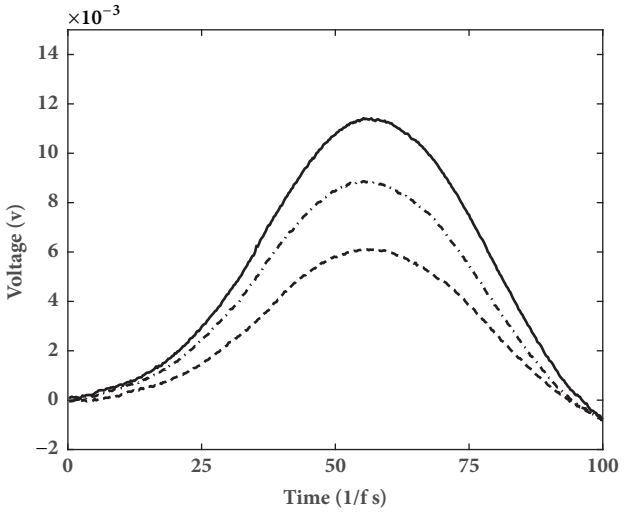

Figure 10: Three raw signal's waveform from different oil droplets.

the height of the sensor was adjusted so as to obtain different velocities of oil droplets, where the equivalent velocities were {1.8787,2.0766, 2.9694, 3.0988 m/s}. The outputs of the corresponding oil droplets at different speeds are shown in Figure 13. It can be seen that the amplitudes of the signals remained almost unchanged, while the pulse width decreased with the increase of speed. Specifically, the experimental result of width was almost in line with the simulation curve in Figure 7, which proved the model very well.

Through the experiments, the correctness of the characteristics of the sensor and the mathematic model was verified. Thus, the debris can be identified by the electrostatic sensor's signal with the parameters of amplitude and pulse width. If there is debris, a signal with a certain amplitude and pulse width will be produced, which may contribute to the changes of some features that can be used to indicate the

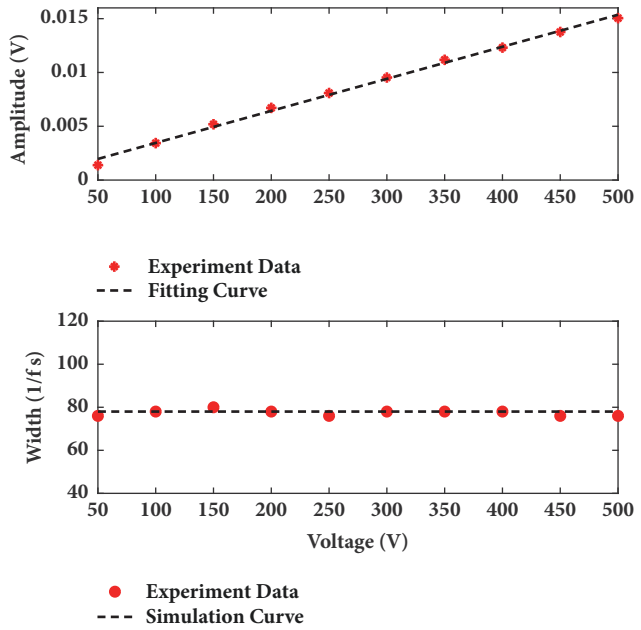

Figure 11: The relationships between outputs and different input charge.

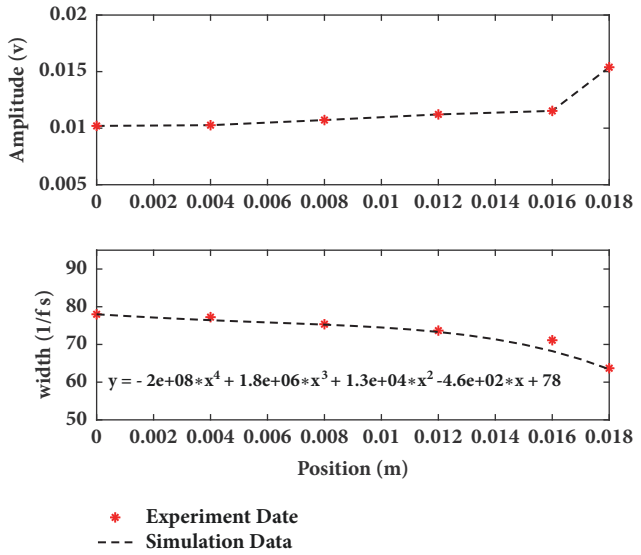

Figure 12: The relationships between the outputs and radial positions.

debris. Therefore, the next part will focus on the feasibility of electrostatic sensors in practical applications and the development of some methods sensitive enough to identify the debris in practical applications.

4. The Debris Recognition Methods and Application in the Gearbox

The verification experiment in the lab proved the correctness of the principle of OLS. However, due to the differences between the industrial environment and the laboratorial

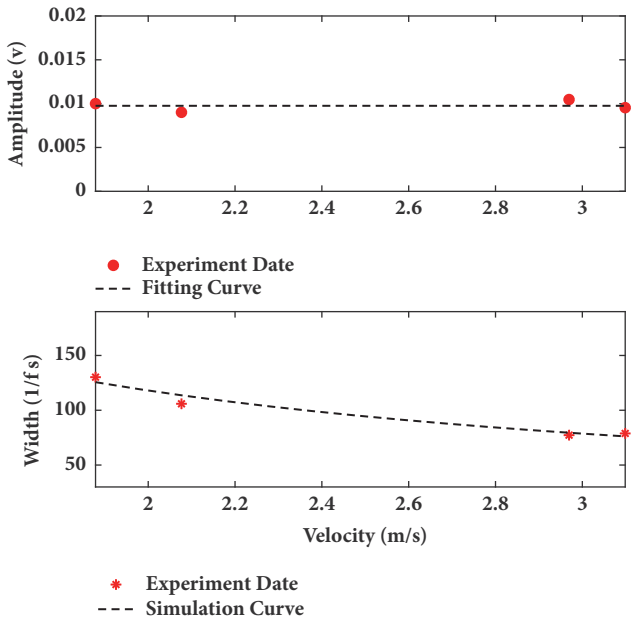

FIGURE 13: The relationships between the outputs and different velocities.

environment, such as the interference problem, in order to further validate the feasibility of the OLS's application in the industrial environment, with a gearbox manufacturer's bench test rig, the experiment on the industrial gearbox were carried out. Meanwhile, two kinds of effective debris recognition methods in the industrial environment were developed to analyze the signals.

4.1. The Test Rig and Test Procedures. The experiment was performed in a practical industrial gearbox bench test rig. As shown in Figure 14, the test rig consists of two practical industrial gearboxes, an electromotor as the drive motor and an electric generator as the loading motor. In the lubricant system of the main test gearbox, two electrostatic sensors integrated into a shielding box and spaced 150 mm apart were mounted in the oil-line of the gearbox to monitor debris produced during testing, aiming to investigate the feasibility of its practical application. The relative locations between the electrostatic sensors and the gearbox in the lubrication system are presented in Figure 14. The electrostatic sensors were installed as close as possible to the gearbox so as to minimize the leakage of the charge on the debris and other influences. After the electrostatic sensors, there was a filter, which could ensure that the debris will no longer enter the oil-line. The diameter and length of the electrostatic sensor probe were 38 mm and 70 mm.

The experiment was a fatigue life test to evaluate the occurrence of wear, pitting and gluing of the tooth surface when the lifetime reached 230 h (13800 min). The input speed, input torque and output torque of the gearbox were 1500 rpm, 4900 Nm and 105000 Nm respectively. The process was divided into four stages and each stage accounted for a quarter of its lifetime. The gear was inspected after each stage. The sensor began to collect the data at the same time when the gearbox started. All data was stored on the computer for further analysis.

4.2. Methods of Debris Recognition Based on Electrostatic Sensors

4.2.1. Method Based on the Amplitude and Pulse Width. According to the characteristics of the debris' signal, the debris can be directly identified by the amplitude and pulse width of the signal. However, in the industrial environment, the interference could be very serious, which may lead to the low accuracy of recognition. Therefore, a new recognition method based on two sensors was developed. As shown in Figure 15, since the two sensors are installed successively in the flow direction, the debris will sequentially induce the characteristic pulse on the two sensors, and the delay time between the pulses is related to the moving speed of the debris and the distance between the two sensors. With the feature of delay time, the results from the two sensors will verify with each other, which is able to exclude the signal fluctuations and other external interference and improve the accuracy of identification further. The specific method is shown in Figure 16.

Step 1. Firstly, to distinguish between the debris signal and the random noise signal, an amplitude threshold is set according to the noise level, and the signal above the threshold is considered to be the potential debris signal.

Step 2. For the signal beyond the amplitude threshold, further identify its peak, and then count the signal sequence backward until 0.1 peak values. The resulting count value multiplied by twice the sampling interval is the pulse width of the debris signal.

Step 3. According to the pulse width, determine whether the signal is caused by debris or interference. For interference, its pulse width is very short, while, for debris, the pulse width has a certain range corresponding to flow rate, which can be determined by the analysis of its model and experiments. The potential debris signal that has the certain range of pulse width is set as the Important Potential Debris Signal (IPDS).

Step 4. Verify the IPDS with the two sensors. As the debris passes orderly through the first sensor and the second sensor, there is a delay time between the occurrence times of the feature signal in the two sensors. By looking for the IPDS in the two sensors within the delay time range, the result can be further confirmed and the final recognition results are obtained.

In the case when multidebris passes the sensor at the same time, the superposition of the signal will cause the pulse width to be widened (out of the range determined by the analysis of its model and experiments) and thus be isolated to provide richer identification information. Here, we use a formula to correct large pulse width signals:

$$\text{Number of debris} = \left\lceil \frac{\text{the measured large width}}{\max(\text{the range of the width})} \right\rceil \quad (9)$$

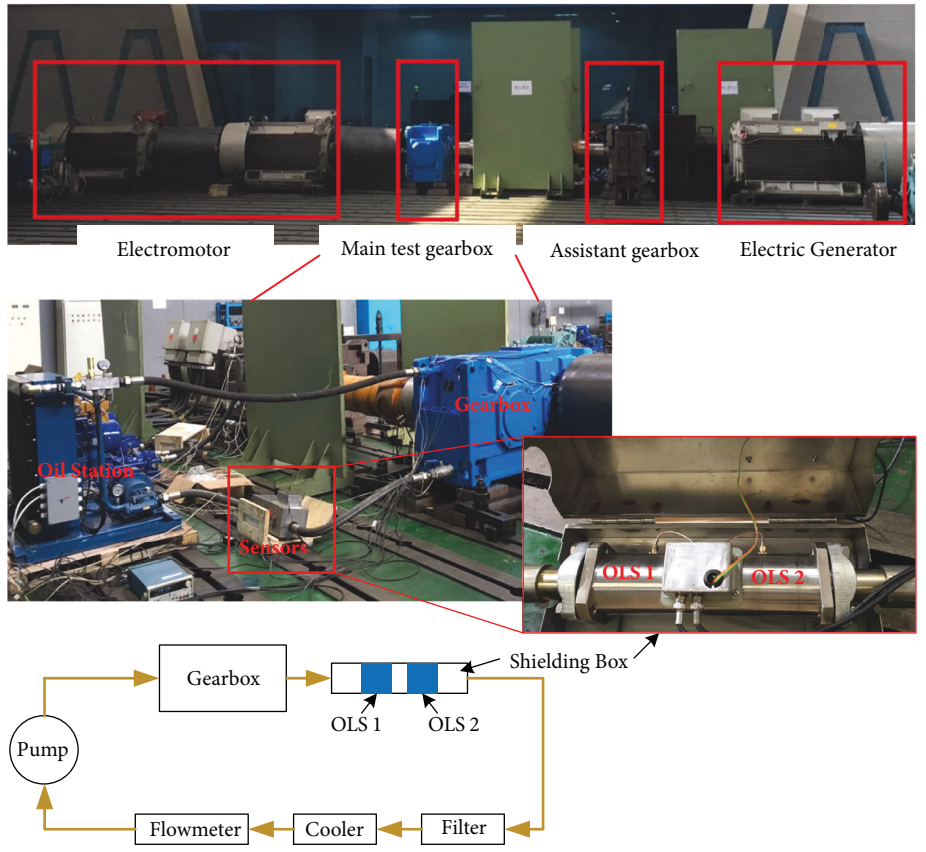

Figure 14: The gearbox test rig.

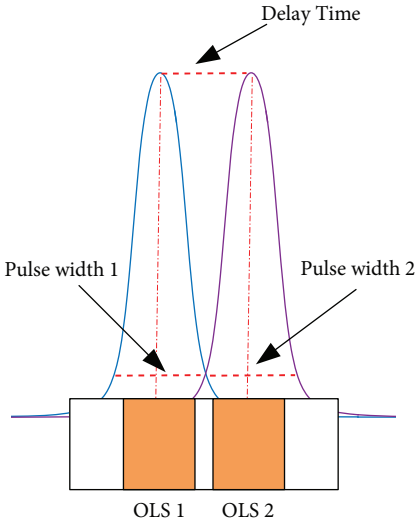

Figure 15: The simulation waveforms on the two sensors induced by the debris.

4.2.2. Method Based on the GEV Distribution. As analyzed above, the debris is correlated to the pulse components in the signal. As the debris pulse will cause the extreme value in the corresponding RMS value, the extreme RMS value can also reflect the debris' generation. General Extreme Value Theory is a branch of statistics concerning data with unusually low or high values, i.e., data that lies in the tails of the distribution [21]. Therefore, this paper proposed a method based on the General Extreme Values (GEV) Distribution, which reflected the information of the debris' generation through the distribution's change.

As shown in Figure 17, the distributions of the extreme RMS value over a period of time from the beginning and end of the experiment can be both well fitted with the General Extreme Values (GEV) Distribution, where the black curve represents the beginning period and the red curve represents the late period. At the beginning, when the gearbox entered a steady working condition, the signal was mainly composed of a background signal, including ambient noise and a certain amount of charge carried by the oil flow. At this point, the extreme RMS value was relatively stable. As shown by the black curve, the tail phenomenon was not obvious, and the distribution was closer to the normal distribution. When the wear occurred, the debris induced the signals with relatively large amplitudes, as described in Sections 2 and 3, and then the tailing phenomenon of the electrostatic signal became very obvious. The detailed algorithm process is as follows:

Step 1. Calculate the RMS value of the signal every 100ms, as the duration time of the pulse in this experiment is around 100ms. Then set the interval to select the extreme value of

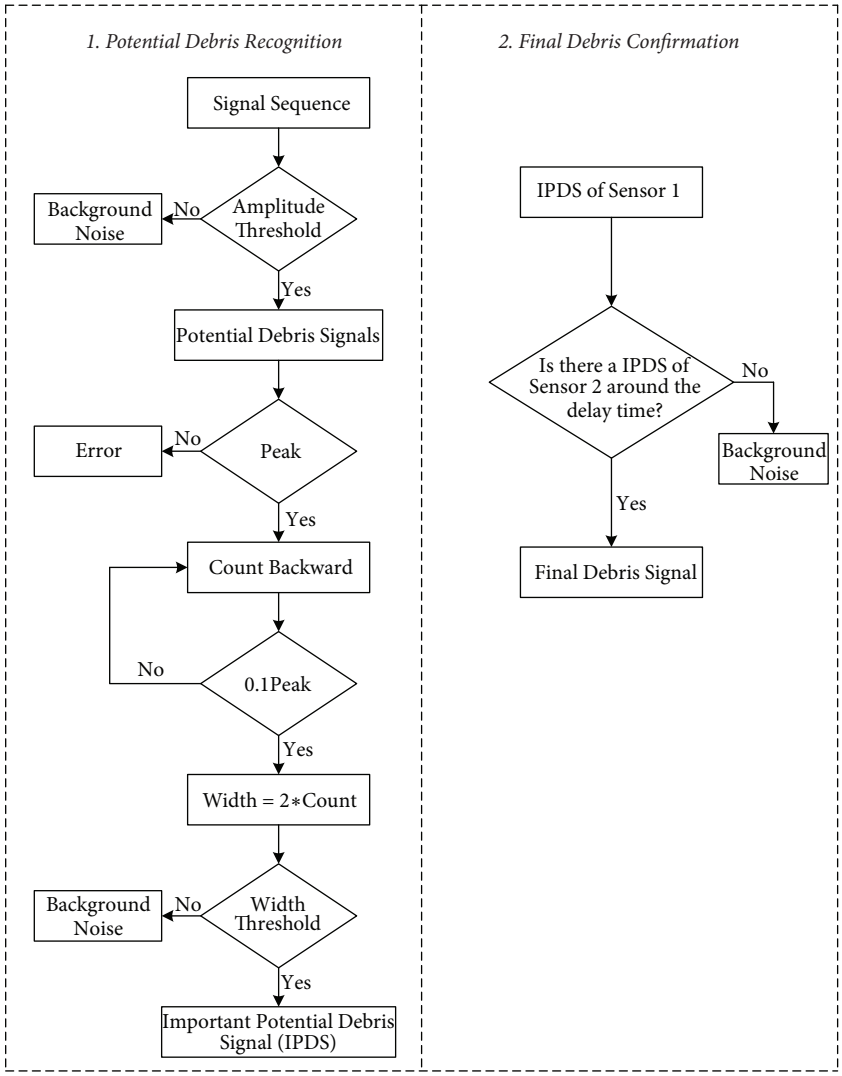

Figure 16: The debris recognition method based on amplitude and pulse width.

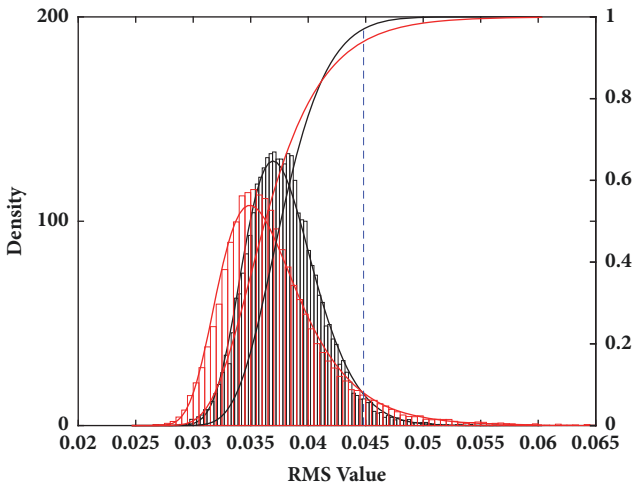

Figure 17: The distribution of the extreme RMS value.

RMS, where the interval is 1s. At last, set a time window width to calculate the extreme value's distribution.

Step 2. Calculate the extreme RMS value's distribution in each time window of the signal sequence. According to the analysis and statistical results, the distribution of the extreme RMS value can be fitted by the GEV distribution.

Step 3. Consider the beginning phase as a default healthy running state, whose distribution can be taken as a reference distribution. Then evaluate the differences between all the distribution with the reference distribution and take the results as an indicator of the occurrence of debris. Specifically, as the blue line shown in the Figure 17, this paper takes the 95th-percentile of the healthy running state as the reference point, calculates the percentage of the points greater than the reference point in the new distribution, and defines the result as confidence value (CV) to evaluate the tail and the

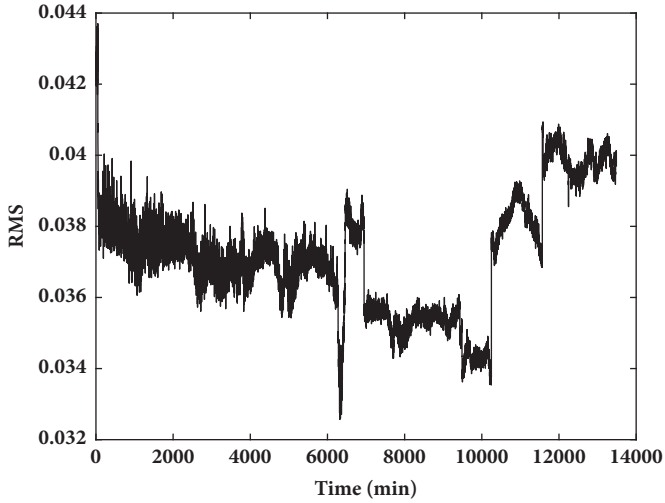

Figure 18: The RMS value of the signal.

difference with the reference distribution, which is able to indicate the occurrence of the debris.

4.3. Results Analysis and Comparison. In this experiment, the inspections of the first two stages (0~3450 min and 3451~6900 min) did not find any failure, but after the third stage (6900~10350 min), a slight pitting within the acceptance range occurred. After the experiment, the inspection found the pitting area expanded. By comparing to the inspection results, the effectiveness of the developed two new debris recognition methods was evaluated. Simultaneously, this part also calculated the RMS value of the signal and the cross-correlation function of the two sensors, which were used by the previous researchers. By comparing the results of all the four methods, the effectiveness of each method was researched.

4.3.1. The RMS Value. The RMS value can indicate the charge level in the oil flow. Over a period of time, the increased amount of debris will make the electrostatic sensor sense more charge, which will also contribute to the higher RMS value. According to this, this method calculated an RMS value of the signal every minute. From the trend of the RMS value and its abnormal change point, some debris information can be extracted. As shown in Figure 18, the RMS started with a very high value, which was considered to be related to the unstable running state of the system at the beginning. After a short time, the RMS value decreased to the relatively steady state. Starting from 6300 min, the RMS value began to fluctuate. At first, it declined sharply, and then rose to and stayed in a certain level. After that, it experienced another sharp decline and decreased to a relatively low level. This phase may be related to the occurrence of the failure. At around 11000 min, the RMS value increased obviously and then stayed at a high level until the end of the experiment.

4.3.2. The Correlation-Based Method. Two electrostatic sensors were used to deduce velocity information related to the oil flow. Typically, this is evidenced by generation of debris, sufficient quantities of which will influence the flow quality monitored by the OLS [7]. By calculating the cross-correlation function between the two signals per minute, the delay time can be extracted and then the speed of the oil flow can be expressed according to the formula:

$$v_{oil} = \frac{D_{sensors}}{t_{dealy}} \tag{10}$$

where v_{oil} means the speed of the oil flow and $D_{sensors}$ means the distance between the two sensors, and t_{dealy} means the delay time. According to the formula, as $D_{sensors}$ remains constant, the delay time can indicate the speed directly. Firstly, a delay time was selected as a threshold according to the normal flow rate, and then any delay time greater than the threshold was identified as suspected debris. Through the statistics of the accumulated suspected debris, the results are shown in Figure 19. The slope of the curve can indicate the generation rate of the debris. It can be seen that in the startup phase, there was not an abnormal phase similar to the RMS value. There were several phases where the slope was high, which usually corresponded to the occurrence of debris caused by failure, such as the period 7800~8200 min, period 11200~11800 min and period 11800~13800 min.

4.3.3. The Method Based on the Amplitude and Pulse Width. The result of this new method is shown in Figure 20. In the initial period 0~1700 min, the generation rate of debris was around 6/min. From 1700 min, the debris level began to decrease and then stayed in around 2/min. At 6300 min, the amount of debris increased rapidly and remained in a relatively high level for about 60 minutes. From 7000 min, the debris increased to a high level again and remained the level until the end. The trend can be interpreted that the initial period 0~1700 min might be related to the 'running-in' period, the phase 1700~6300 min possibly corresponded to the stable operation stage, and the time 6300 min could be the moment failure occurred.

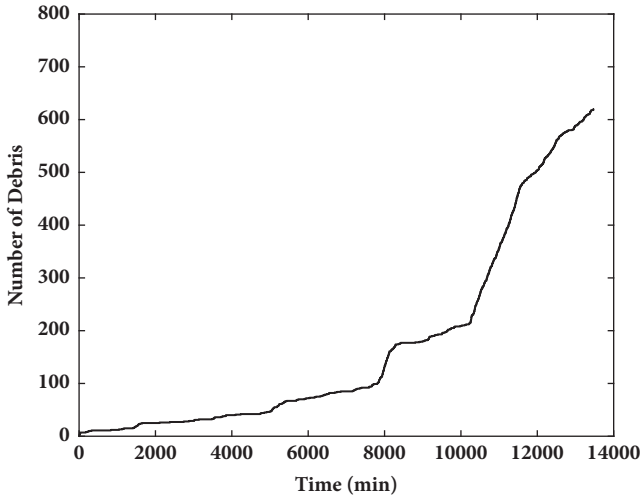

Figure 19: The accumulated number of debris calculated by cross-correlation function.

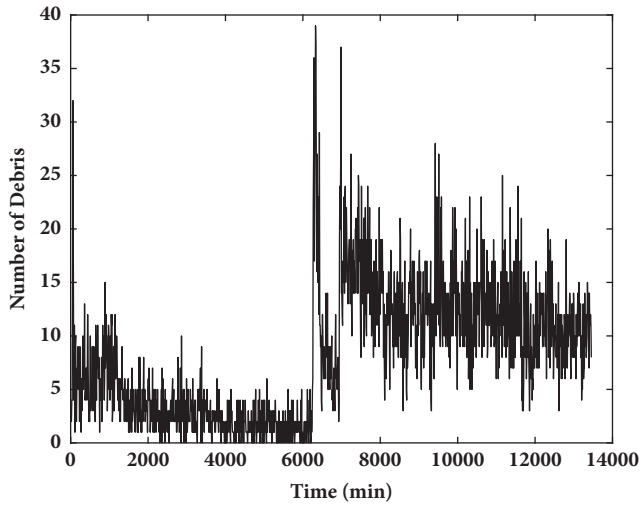

Figure 20: The amount of debris per minute counted by pulse width.

Compared with the correlation-based method, the debris information extracted by the pulse width is more detailed. The correlation-based method can only calculate the correlation coefficient over a period of time, which means it can only characterize the presence of debris for a period of time instead of identifying the amount of debris. However, through the pulse width, all the potential debris can be identified. Thus, it can provide more information, such as severity of wear.

4.3.4. GEV Distribution-Based Method. The results of this method are shown in Figures 21 and 22. Figure 21 represents the mean value of every GEV distribution, the trend of which is very similar to that of RMS value in Figure 18. Figure 22 shows the trend of CV. In the initial period 0~1800 min, CV remained stable. However, after 1800 min, CV decreased rapidly and then stayed around a very low level until 6300 min, which corresponded to the stable operation phase of gearbox. At around 6300 min, there was a sudden rise and

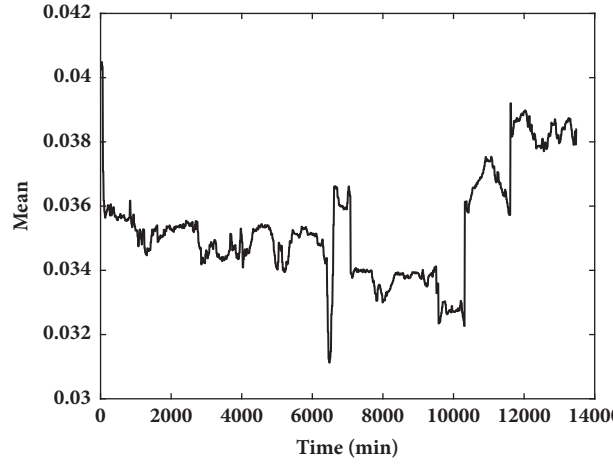

Figure 21: The trend of the mean value.

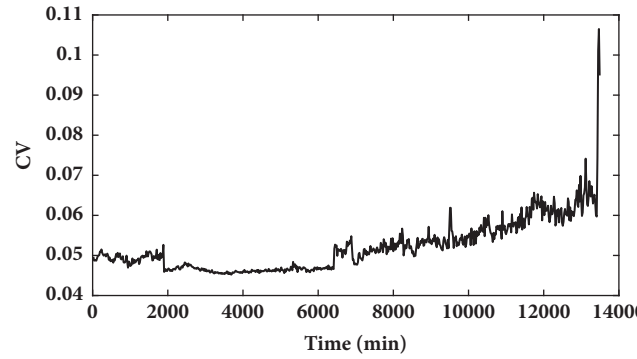

Figure 22: The trend of CV.

then it stayed in a relatively high level for nearly 500 minutes and then dropped again. After this period, the CV increased persistently and ended with a very high value.

To summarize, only the pulse width-based method and the GEV distribution-based method can indicate the running-in phase lying between around 0~1800 min. During the period 2000~6000 min, all the results of the four methods remained stable, which may correspond to the stable operation period. Beginning at around 6300 min, three methods except the correlation-based method experienced the abnormal increase successively, which was considered to be related to the occurrence of the initial fault. Until 7800 min, the correlation-based method monitored its first anomaly. However, the inspection after the second stage (3451~6900 min) didn't find any fault, the reason of which might be that the fault was in its early stage and cannot be distinguished by the naked eye. Then, the RMS value (7200~11000 min) and correlation-based method (8200~11200 min) underwent a relatively stable phase, but the results identified by the pulse width and the GEV distribution continued to indicate debris, which may be related to the fine debris in this stage. From around 11000 min, all methods had an upward trend correspond to the failure, which were also proved by the final inspections.

Among the four methods, RMS can indicate the overall charge level in the oil-line, but cannot indicate the instantaneous generation of the debris. Moreover, since the charge sources in the oil are complex, the OLS signals and its RMS value are susceptible. The GEV distribution-based method is an improvement of the RMS-based method. The mean value of the GEV distribution can show the trend of the overall charge, which is similar to the RMS value. However, in addition, the GEV distribution can also reflect the changes of the extreme value in the signal, which is usually corresponding to the debris. Therefore, the GEV distribution-based method can indicate the debris better in each period. RMS-based method and GEV distribution-based method are both based on the statistical analysis of OLS signals to reflect the debris indirectly. While the cross-correlation-based methods and pulse waveform-based methods are intended to directly identify the debris. For the correlation-based method, because of its principle, it is ineffective for fine debris monitoring and situations where the amount of debris is low. What's more, the correlation-based method can only judge if there is debris occurring in the period of time, but the amount of debris can't be identified. The experimental results also showed the information obtained by the correlation-based indicator was much less than that of the other three methods. The method of pulse width can identify all the debris theoretically by directly recognizing the amplitude and pulse width of the debris signal. The experimental results proved the effectiveness of this method. Compared to the GEV distribution, the method based on identifying the pulse width is more direct in debris recognition and better in real time, but the GEV distribution can provide the information about the overall charge of the oil flow.

5. Conclusions

This paper further researched the OLS by detailing the characteristics of the sensor and developing two more reasonable and precise debris recognition methods based on the characteristics of the sensor. Through developing the detailed mathematical model of the OLS, this paper proved that the amplitude and pulse width of the signal could be used to indicate the debris and their change rules were obtained as the characteristics of the sensor. Then a new OLS test rig was developed, which creatively used an oil drop charge device to simulate the charged debris. The OLS test rig verified the correctness of the mathematical model and the characteristics of the OLS, the experimental width data of which could fit the simulation data very well. The practical application of OLS in the gearbox evaluated the feasibility of OLS and the two new debris recognition methods. Compared to the traditional methods, the new methods were proved to be able to provide more information of debris and improve the sensor detection capability.

However, as the proposed methods use the raw signals in the time domain directly, only the signals from the stable working conditions of the gearbox can be used so as to ensure the accuracy of the recognition result. In addition, the methods put forward in this paper only focused on the identification of the occurrence and the amount of debris, whereas the morphological information was not involved too much. In the future, the relationships between the signals and the size, the material properties, and other morphological information will be further studied, which can make the electrostatic more effective on fault diagnosis.

Data Availability

The experimental data used or analyzed during the current study are available from the corresponding author on reasonable request.

Conflicts of Interest

The authors declare no conflicts of interest.

Acknowledgments

This work was supported in part by Major Program of Civil Aviation Joint Funds of China (U1733201) and Jiangsu Scientific Research Innovation Plan (KYCX 16-0386).

References

[1] J. Vižintin, J. Salgueiro, G. Peršin, and Đ. Juričić, "System for automated online oil analysis," *Condition monitor*, vol. 336, pp. 5–10, 2015.

[2] J. Luo, D. Yu, and M. Liang, "Enhancement of oil particle sensor capability via resonance-based signal decomposition and fractional calculus," *Measurement*, vol. 76, pp. 240–254, 2015.

[3] C. Li, J. Peng, and M. Liang, "Enhancement of the wear particle monitoring capability of oil debris sensors using a maximal overlap discrete wavelet transform with optimal decomposition depth," *Sensors*, vol. 14, no. 4, pp. 6207–6228, 2014.

[4] C. Li and M. Liang, "Separation of the vibration-induced signal of oil debris for vibration monitoring," *Smart Materials & Structures*, vol. 20, no. 4, Article ID 045016, 2011.

[5] T. J. Harvey, R. J. K. Wood, and H. E. G. Powrie, "Electrostatic wear monitoring of rolling element bearings," *Wear*, vol. 263, no. 7-12, pp. 1492–1501, 2007.

[6] S. Morris, R. J. K. Wood, T. J. Harvey, and H. E. G. Powrie, "Use of electrostatic charge monitoring for early detection of adhesive wear in oil lubricated contacts," *Journal of Tribology*, vol. 124, no. 2, pp. 288–296, 2002.

[7] O. D. Tasbaz, R. J. K. Wood, M. Browne, H. E. G. Powrie, and G. Denuault, "Electrostatic monitoring of oil lubricated sliding point contacts for early detection of scuffing," *Wear*, vol. 230, no. 1, pp. 86–97, 1999.

[8] H. E. G. Powrie and C. E. Fisher, "Engine health monitoring: towards total prognostics," *IEEE Aerospace Applications Conference Proceedings*, vol. 3, pp. 11–20, 1999.

[9] H. Powrie, "Use of electrostatic technology of aero engine oil system monitoring," in *Proceedings of the 2000 IEEE Aerospace Conference*, pp. 57–72, USA, March 2000.

[10] H. Powrie, C. E. Fisher et al., "Performance of an electrostatic oil monitoring system during an FZG gear scuffing test," in *Proceedings of the International Conference on Condition Monitoring*, pp. 145–155, University of Wales Swansea, Swansea, UK, April 1999.

[11] T. J. Harvey, S. Morris, L. Wang, R. J. K. Wood, and H. E. G. Powrie, "Real-time monitoring of wear debris using electrostatic sensing techniques," *Proceedings of the Institution of Mechanical Engineers, Part J: Journal of Engineering Tribology*, vol. 221, no. 1, pp. 27–40, 2007.

[12] T. J. Harvey, R. J. K. Wood, G. Denuault, and H. E. G. Powrie, "Effect of oil quality on electrostatic charge generation and transport," *Journal of Electrostatics*, vol. 55, no. 1, pp. 1–23, 2002.

[13] T. J. Harvey, R. J. K. Wood, H. E. G. Powrie, and C. Warrens, "Charging ability of pure hydrocarbons and lubricating oils," *Tribology Transactions*, vol. 47, no. 2, pp. 263–271, 2004.

[14] L. Wang, R. J. K. Wood, I. Care, and H. E. G. Powrie, "Electrostatic wear sensing of ceramic-steel lubricated contacts," *Tribology and Interface Engineering Series*, vol. 43, pp. 711–720, 2004.

[15] H. Powrie, R. Wood, T. Harvey, L. Wang, and S. Morris, "Electrostatic charge generation associated with machinery component deterioration," in *Proceedings of the 2002 IEEE Aerospace Conference*, pp. 2927–2934, USA, March 2002.

[16] Z. Chen, X. Tang, Z. Hu, and Y. Yang, "Investigations into sensing characteristics of circular thin-plate electrostatic sensors for gas path monitoring," *Chinese Journal of Aeronautics*, vol. 27, no. 4, pp. 812–820, 2014.

[17] T. Addabbo, A. Fort, M. Mugnaini, E. Panzardi, and V. Vignoli, "A Smart Measurement System with Improved Low-Frequency Response to Detect Moving Charged Debris," *IEEE Transactions on Instrumentation and Measurement*, vol. 65, no. 8, pp. 1874–1883, 2016.

[18] S. Zhang, Y. Yan, and X. Qian, "Mathematical modeling and experimental evaluation of square-shaped electrostatic sensor arrays for gassolid two-phase flowmeasurement," *Zhongnan Daxue Xuebao*, p. 49, 2018.

[19] H. Mao, H. Zuo, and H. Wang, "Electrostatic Sensor Application for On-Line Monitoring of Wind Turbine Gearboxes," *Sensors*, vol. 18, no. 10, p. 3574, 2018.

[20] S. L. Chen, R. J. K. Wood, L. Wang et al., "Wear detection of rolling element bearings using multiple-sensing technologies and mixture-model-based clustering method," *Proceedings of the Institution of Mechanical Engineers, Part O: Journal of Risk and Reliability*, vol. 2, pp. 207–218, 2008.

[21] S. Chen, M. Craig, R. Callan, H. Powrie, and R. Wood, "Use of Artificial Intelligence Methods for Advanced Bearing Health Diagnostics and Prognostics," in *Proceedings of the 2008 IEEE Aerospace Conference*, pp. 1–9, Big Sky, MT, USA, March 2008.

[22] T. J. Harvey, R. J. K. Wood, G. Denuault, and H. E. G. Powrie, "Investigation of electrostatic charging mechanisms in oil lubricated tribo-contacts," *Tribology International*, vol. 35, no. 9, pp. 605–614, 2002.

[23] G. Stachowiak and A. W. Batchelor, *Engineering Tribology*, Butterworth-Heinemann, 2013.

[24] M. Rossner and H. Singer, "Measurement of micrometer particles by means of induced charges," in *Proceedings of the Conference Record of the 1989 IEEE Industry Applications Society Annual Meeting - Presented at the 24th IAS Annual Meeting.Part II*, pp. 2233–2238, October 1989.

[25] S. L. Carnie and G. M. Torrie, "The Statistical Mechanics of the Electrical Double Layer," in *Advances in Chemical Physics*, Advances in Chemical Physics, pp. 141–253, John Wiley & Sons, Inc., Hoboken, NJ, USA, 1984.

[26] N. C. Sahoo, M. M. A. Salama, and R. Bartnikas, "Trends in partial discharge pattern classification: a survey," *IEEE Transactions on Dielectrics and Electrical Insulation*, vol. 12, no. 2, pp. 248–264, 2005.

[27] T. Addabbo, A. Fort, R. Garbin, M. Mugnaini, S. Rocchi, and V. Vignoli, "Theoretical characterization of a gas path debris detection monitoring system based on electrostatic sensors and charge amplifiers," *Measurement*, vol. 64, pp. 138–146, 2015.